Journal of Medicinal Chemistry
Brief Article

J. Med. Chem. **2010,** *53,* 7461–7465 **7461**
DOI: 10.1021/jm1007159

An *o*-Aminoanilide Analogue of 1α,25-Dihydroxyvitamin D_3 Functions as a Strong Vitamin D Receptor Antagonist

Marc Lamblin,[†] Russell Spingarn,[‡] Tian-Tian Wang,[‡] Melanie C. Burger,[†] Basel Dabbas,[‡] Nicolas Moitessier,[†] John H. White,*[,‡,§] and James L. Gleason*[,†]

Departments of [†]Chemistry, [‡]Physiology, and [§]Medicine, McGill University, Montreal, Quebec, H3A 2K6, Canada

Received June 16, 2010

Vitamin D receptor (VDR) antagonists have therapeutic potential in treatment of allergic conditions and hypercalcemia driven by granulomatous diseases. We have identified an *o*-aminoanilide analogue of the hormonal form of vitamin D with a dienyl side chain that functions as a strong VDR antagonist. Modeling studies indicate that antagonism arises from side chain rigidity, when compared to a more flexible saturated analogue, which interferes with H12 folding/alignment.

Introduction

The hormonal form of vitamin D_3, 1α,25-dihydroxyvitamin D_3 (1,25D,[a] **1**) (Chart 1) has long been known for its central role in controlling calcium homeostasis. More recently, data from several sources have provided evidence that endogenous 1,25D has cancer chemopreventive properties and that it functions as a key regulator of innate and adaptive immune responses.[1,2] As the therapeutic activity of exogenously administered 1,25D is limited by its capacity to induce hypercalcemia, numerous laboratories have developed a wide range of 1,25D analogues that retain VDR agonism but minimize its calcemic actions.[3] In contrast, only a small number of VDR antagonists have been reported, and of these most are only partial antagonists.[4] VDR antagonists have therapeutic potential in modulation of allergic responses[5] and in suppression of hypercalcemia associated with excessive macrophage action in granulomatous diseases such as sarcoidosis.[6]

We have been interested in developing bifunctional 1,25D analogues that combine VDR agonism with histone deacetylase (HDAC) inhibitory activity,[7,8] as both 1,25D and HDACs are modulators of gene transcription and have potential in cancer therapy. HDAC inhibitors (HDACi) such as trichostain A (TSA, **2**) (Chart 1) contain terminal zinc binding groups such as hydroxamic acids. In the bifunctional analogue triciferol (**3**), the side chain of the 19-nor analogue of **1**[9] is replaced by the dienylhydroxamic acid of **2**. Detailed biochemical studies showed that **3** is a VDR agonist and HDACi.[7] We have since developed a range of analogues possessing alternative terminal zinc binding groups including *o*-aminoanilides, thioglycloates, and sulfonamides.[8] Notable among these second-generation hybrid molecules was *o*-aminoanilide ML 2-250 (**4**),[8] which retained significant VDR agonism even with a sterically demanding *o*-aminoanilide group at the side chain terminus. Here we show that a minor structural change, reverting to the dienyl side chain found in TSA and triciferol in place of the saturated side chain, transforms agonist **4** into strong VDR antagonist ML 3-452 (**5**).

Chart 1. 1,25D, TSA, and 1,25D Analogues

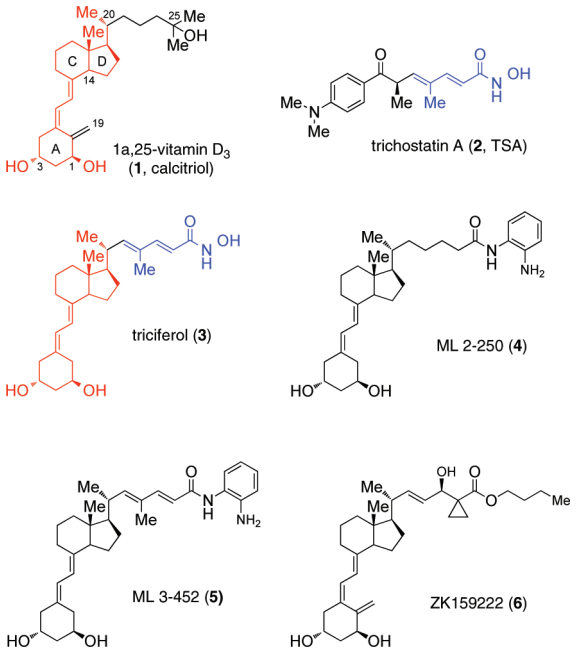

Results and Discussion

VDR antagonist **5** was synthesized following the procedure described for **3**, with *o*-aminoanilide formation replacing hydroxamic acid formation (see Supporting Information for synthetic scheme). The agonist activity of **1**, **4**, and **5** was compared in a 1,25D-sensitive squamous carcinoma cell line SCC25[10] by screening for induction of the *CYP24* gene which

*To whom correspondence should be addressed. For J.H.W.: phone, 514-398-8498; fax, 514-398-7452; e-mail, john.white@mcgill.ca. For J.L.G.: phone, 514-398-5596; fax, 514-398-3797; e-mail, jim.gleason@mcgill.ca.

[a] Abbreviations: VDR, vitamin D receptor; VDR-LBD, vitamin D receptor ligand binding domain; HDAC, histone deacetylase; HDACi, histone deacetylase inhibitor; 1,25D, 1,25-dihydroxyvitamin D_3; TSA, trichostatin A; TSLP, thymic stromal lymphoprotein; PCR, polymerase chain reaction; qPCR, quantitative polymerase chain reaction; MD, molecular dynamics; rmsd, root mean square deviation.

© 2010 American Chemical Society

Published on Web 09/30/2010

encodes the enzyme that initiates metabolism of **1**. Hybrid **5** (1 μM, Figure 1a) induced substantially less *CYP24* expression than a suboptimal concentration of **1** (10 nM) or **4** (1 μM). Similarly, **5** (1 μM) failed to induce transcription of the gene encoding thymic stromal lymphoprotein (TSLP), whereas *TSLP* expression was strongly stimulated by **1** (100 nM, Figure 1b). Direct binding of **5** to the VDR was tested by a fluorescence polarization competition assay[7] using a fluorescent tracer bound to the purified VDR ligand binding domain. These studies (Figure 1c) confirmed that **5** bound directly to the VDR ligand binding domain and displaced the bound tracer with an estimated IC_{50} of 107 nM, or about 8-fold less potently than **1** in this assay. For comparison, agonist **4** binds to the VDR with an IC_{50} of 248 nM, approximately 2.5 times weaker than **5**, yet shows clear dose-dependent induction of *CYP24* expression in SCC25 cells.[8]

The lack of significant *CYP24* and *TSLP* expression coupled with the affinity of **5** for the VDR raised the possibility that it could act as an antagonist for the receptor. Returning to gene expression, analysis by semiquantitative and real-time PCR showed that **5** blocked *CYP24* induction by **1** (10 nM), with substantial inhibition observed at concentrations as low as 100 nM (Figure 2). Again, no substantial CYP24 expression was observed in the presence of **5** (1−10 μM) as measured by semiquantitative or qPCR. We further compared antagonist **5** with established antagonist ZK159222 (**6**).[3] **6** appeared to be a more potent antagonist than **5** (Figure 2b). However, in contrast to **5**, **6** induced measurable *CYP24* expression (Figure 2).

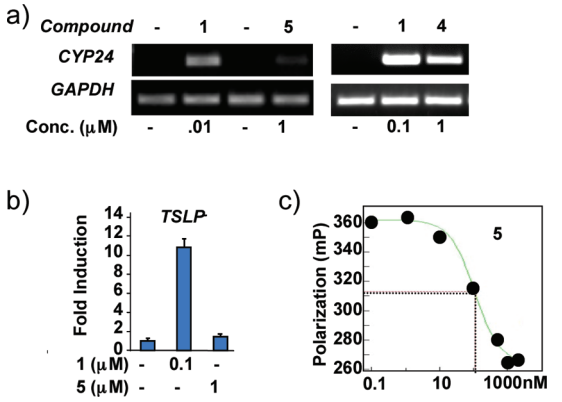

Figure 1. Expression of (a) CYP24 and (b) TSLP in SCC25 cells, as monitored by CYP24, indicates no VDR agonism by *o*-aminoanilide **5**. GAPDH is used as a control. (c) A fluorescence polarization assay of hybrid **5** shows binding to the VDR with an IC_{50} of 107 nM.

In the presence of **1**, the DNA-bound VDR activates transcription in part by recruiting coactivator proteins to promoter regions of target genes.[1] Unlike **1**, **5** failed to induce association of the VDR coactivator AIB1 with the vitamin D-responsive region of the *CYP24* promoter and blocked AIB1 recruitment induced by **1**, as assessed by chromatin immunoprecipitation (ChIP) assay (Figure 3).[7] Moreover, in a similar assay, **5** partially induced association of corepressor NCoR with the *CYP24* promoter, whereas **1** suppressed NCoR binding (Figure 3), further substantiating function of **5** as an antagonist.

Intriguingly, in addition to its different action on the VDR, hybrid **5** also is devoid of the HDACi activity of **4**. Treatment of SCC4 cells with **5** (1 μM) did not induce hyperacetylation of histone H4 or tubulin as judged by Western blotting. This is in contrast to **4** which induces histone H4 and tubulin hyperacetylation at equivalent concentrations.[8] Moreover, no inhibition of purified recombinant human HDAC6 by **5** was observed up to 1 mM using a standard fluorescence assay.[11] Again, by contrast, hybrid **4** inhibits HDAC6 with an IC_{50} of 81 μM.[8]

The VDR antagonist activity of **5** is striking given the agonist action of **4** and **3**. Antagonism of the VDR is usually suggested to arise by destabilization of the required positioning of H12 that forms part of a crucial recognition element for coactivator recruitment.[4b,g,12] To gain insight into the differing effects of **4** and **5** on the VDR, we modeled their interactions using virtual docking and molecular dynamics simulations. We employed FITTED 2.6, a suite of programs for virtual screening.[13] Visual inspection of the docked poses to the full-length VDR X-ray structure[14] revealed that **4** may

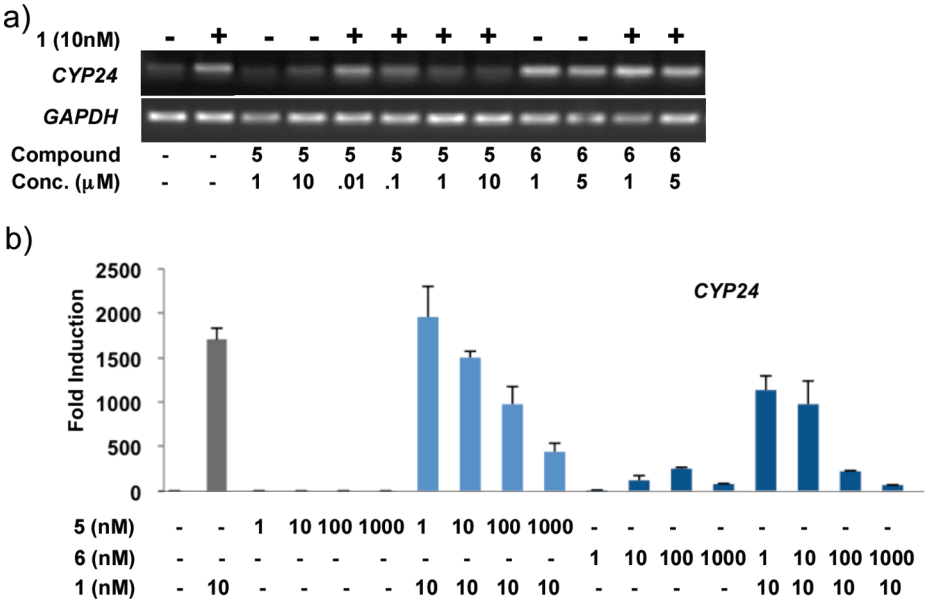

Figure 2. Semiquantitative (a) or qPCR (b) analysis of *CYP24* regulation in SCC25 cells. Clear dose-dependent inhibition of expression induced by 1,25D (**1**) and no substantial agonism of *o*-aminoanilide (**5**) were observed over 0.01−10 μM. Analysis of the partial agonist and antagonist activity of **6** is provided for comparison.

stabilize the agonist conformation through a hydrogen bonding interaction between the *o*-aminoanilide and histidine 395 on helix 11 (H11). The repositioning of H11 so that it is contiguous with H10 is required for folding over of H12 to generate an agonized conformation of the VDR.[15] Conversely **5** was unable to orient the *o*-aminoanilide to interact with His395 in an agonized conformation of the VDR (Figure 4b).[16]

The only X-ray crystal data available for VDR antagonists are structures that have been cocrystallized with coactivator peptides, which presumably leads to an active conformation of the receptor.[4g,h] To mimic an inactive conformation of the receptor, we truncated the 1,25D-liganded VDR[14] by removing H12. When docked to this structure, the side chains of **4** and **5** extended into the volume previously occupied by H12 (Figure 4). However, when energies of binding are compared to those of the full and truncated VDR, an energy benefit of −20 kcal/mol was observed for **5**, which was considerably stronger than that observed for **4** (−6 kcal/mol). The larger energy difference is partially accounted for by loss of syn-pentane and A-1,3 strain in the extended conformation of **5** and suggests that it is much less tolerant of compaction into the ligand binding pocket and may significantly hinder proper positioning of H12.[17]

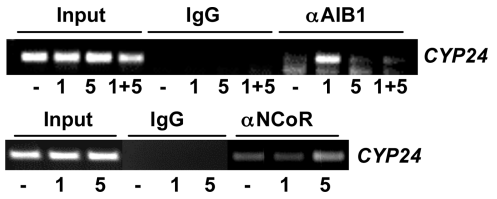

Figure 3. ChIP analysis of the effects of **1** (10 nM) or **5** (1 μM) alone or in combination on the association of VDR coactivator AIB1 (top) or corepressor NCoR (bottom) with the VDR binding region of the proximal promoter of the *CYP24* gene.

To further examine the potential influence of **5** on H12, we compared effects of **1**, **4**, and **5** bound to VDR in molecular dynamics (MD) simulations using Amber 10 (Figure 5).[12a,18] MD simulation of VDR complexes of **1** and **4** over a 40 ns time frame showed minor variations in the position of H12 residues. In the case of **4**, H12 closed very slightly over the binding pocket during the time frame we examined, while with **1**, H12 fluctuated insignificantly about the average agonist conformation. In the case of antagonist **5**, H12 was displaced slightly away from the binding pocket during the first portion of the simulation. More strikingly, during the second half of the simulation, H12 began to partially unwind. This change is most readily apparent by observing the movement of the side chains of Glu420, Val421, and Phe422 (Figure 5c), the last of which is displaced with an rmsd of 5.26 Å (vs 1.43 Å for **1** and 2.26 Å for **4**). This is considerable movement over a short time frame and suggests the potential to completely displace H12 over the time frame normally expected for movement of larger subunits (on the order of seconds). This movement also

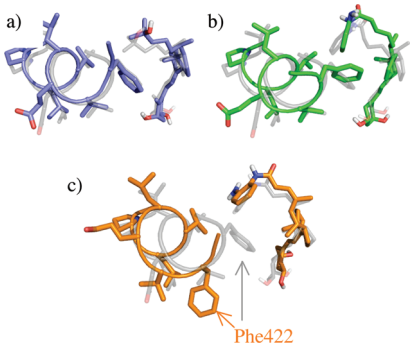

Figure 5. Molecular dynamics simulations showing initial positions (in gray) of ligands (right) and H12 (left) and final positions of ligands and H12 (in color) after 40 ns for (a) 1,25D (**1**), (b) agonist **4**, and (c) antagonist **5** showing significant movement and partial unwinding of H12 induced by **5**.

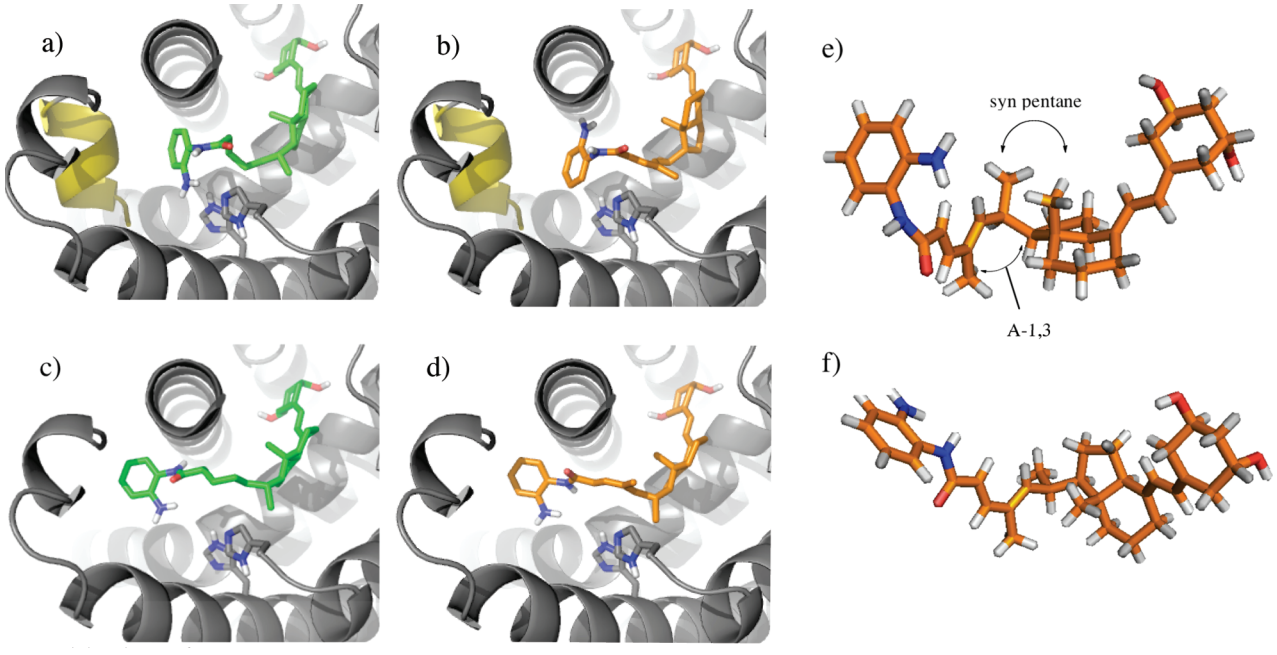

Figure 4. Docking of (a) agonist **4** and (b) antagonist **5** to VDR-LBD showing hydrogen bonding in the former. Docking of (c) agonist **4** and (d) antagonist **5** to VDR-LBD lacking H12 indicates a preference for both ligands for an extended conformation. Extracted conformation of agonist **5** bound to (e) VDR-LBD and (f) VDR-LBD lacking H12 shows relief of syn-pentane and A-1,3 interactions in H12 deleted structure.

significantly affected the distance between Lys248 and Glu420 that form a charge clamp for coactivator binding. For **1** and **4**, this distance varied between 18 and 19.6 Å during the course of the simulation, while for **5**, the distance increased substantially to 21.5 Å at the end of the simulation. Taken together, the MD and docking studies suggest that the relative rigidity and propensity to avoid internal A-1,3 strain of LBD-bound **5** make it more difficult for H12 to be properly positioned within the VDR to allow efficient coactivator binding, thus leading to an inactive holo-VDR and explaning the antagonistic effect of **5** on **1** when present in concentrations high enough to compete effectively for binding.

Conclusion

We have identified an *o*-aminoanilide analogue of 1,25D that is a potent antagonist of the VDR. The antagonistic activity appears to arise because of a more rigid side chain, which inhibits the alignment of H12 necessary for coactivator binding to the VDR.

Experimental Section

((*R*,2*E*,4*E*)-6-((1*R*,3a*S*,7a*R*,*E*)-4-(2-((3*R*,5*R*)-3,5-Bis(*tert*-butyldimethylsilyloxy)cyclohexylidene)ethylidene)-7a-methyloctahydro-*1H*-inden-1-yl)-4-methylhepta-2,4-dienoic Acid (7). $LiOH \cdot H_2O$ (4.8 mg, 0.114 mmol, 3 equiv) was added to a stirring solution of methyl-(2*E*,4*E*,6*R*)-6-((1*R*,3*R*,7*E*,17β)-1,3-bis[*tert*-butyl(dimethyl)silyloxy]-9,10-secoestra-5,7-dien-17-yl)-4-methylhepta-2,4-dienoate[7] (25.5 mg, 0.038 mmol) in THF (0.5 mL), MeOH (200 μL), and H_2O (200 μL). The reaction vessel was fitted with a reflux condenser, and the mixture brought to reflux for 3 h via a heating mantle. The mixture was cooled to room temperature and diluted with EtOAc (5 mL), then quenched with a 1.0 M solution of HCl (5 mL). The layers were separated, and the aqueous layer was further extracted with EtOAc (2 × 5 mL). The organic layers were combined and extracted with distilled H_2O (5 mL) and brine (5 mL), then dried ($MgSO_4$), and concentrated in vacuo to give the crude product. The acid was carried forward without further purification. Quantitative yield was 24.4 mg, 0.038 mmol. R_f = 0.30 (20% EtOAc in hexanes); ^{1}H NMR (300 MHz, $CDCl_3$) δ 10.00−9.30 (1H, br s), 7.39 (1H, d, J = 15.5 Hz), 6.16 (1H, d, J = 11.0 Hz), 5.82 (2H, m), 5.78 (1H, d, J = 15.5 Hz), 4.15−4.00 (2H, m), 2.87−2.78 (1H, m), 2.63−2.53 (1H, m), 2.44−2.24 (3H, m), 2.16−1.96 (3H, m), 1.83 (3H, s), 1.82−1.36 (11H, m), 1.04 (3H, d, J = 6.5 Hz), 0.89 (9H, s), 0.88 (9H, s), 0.60 (3H, s), 0.06 (12H, m); ^{13}C NMR (75 MHz, $CDCl_3$) δ 173.1, 152.7, 149.8, 140.3, 134.0, 129.9, 121.7, 116.5, 114.8, 68.3, 68.1, 56.6, 56.3, 46.2, 46.0, 43.9, 40.7, 37.1, 36.4, 28.9, 27.5, 26.1 (6C), 23.6, 22.5, 20.1, 18.4 (2C), 12.9, 12.7, −4.3, −4.4, −4.5, −4.6; IR (film) ν 3000 (br), 2956, 1686, 1618, 1417, 1254, 1207, 1088, 1026, 908, 834, 801 cm^{-1}. HRMS (ESI) m/z calcd for [(M + H)$^+$], 643.4578; found, 643.4570.

(*R*,2*E*,4*E*)-*N*-(2-Aminophenyl)-6-((1*R*,3a*S*,7a*R*,*E*)-4-(2-((3*R*,5*R*)-3,5-bis(*tert*-butyldimethylsilyloxy)cyclohexylidene)ethylidene)-7a-methyloctahydro-*1H*-inden-1-yl)-4-methylhepta-2,4-dienamide (8). HBTU (7.9 mg, 0.021 mmol, 1.1 equiv) was added to a solution of acid **7** (12.2 mg, 0.019 mmol, 1 equiv), 1,2-phenylenediamine (2.0 mg, 0.019 mmol, 1 equiv), HOBt (7.7 mg, 0.095 mmol, 5 equiv), and DIPEA (9.9 μL, 0.057 mmol, 3 equiv) in DMF (190 μL). The mixture was stirred at room temperature for 1 h, then diluted with EtOAc (10 mL). The organic solution was washed with saturated $NaHCO_3$ (5 mL), water (5 mL), brine (5 mL) and dried (Na_2SO_4). The solution was filtered, concentrated, and the oil was purified by silica gel chromatography (10−30% EtOAc in hexanes) to provide **8** as a clear oil in 86% yield (12 mg, 0.016 mmol). R_f = 0.6 (40% EtOAc in hexanes); ^{1}H NMR (400 MHz, $CDCl_3$) δ 7.35 (1H, d, J = 15.2 Hz), 7.23 (2H, brs), 7.06 (1H, d, J = 7.6 Hz), 6.16 (1H, d, J = 11.2 Hz), 5.92 (1H, d, J = 14.8 Hz), 5.80 (1H, d, J = 11.2 Hz), 5.72 (1H, d, J = 10.0 Hz), 4.10−4.02 (2H, m), 3.94 (1H, brs), 2.81 (1H, d, J = 12.0 Hz), 2.55 (1H, d, J = 6.8 Hz), 2.40−2.31 (2H, m), 2.26 (1H, d, J = 12.8 Hz), 2.10 (1H, dd, J = 12.8, 8.0 Hz), 2.05−1.95 (2H, m), 1.87−1.30 (16H, m), 1.13 (1H, brs), 1.02 (3H, d, J = 6.4 Hz), 0.87 (9H, s), 0.57 (9H, s), 0.58 (3H, s), 0.05 (12H, s); ^{13}C NMR (75 MHz, $CDCl_3$) δ 165.3, 148.5, 141.1, 140.6, 134.1, 129.6, 128.5, 127.2, 125.3, 124.8, 121.9, 119.8, 118.5, 117.6, 116.5, 68.3, 68.2, 56.6, 56.3, 46.2, 45.9, 43.9, 40.7, 37.1, 36.3, 28.9, 27.4, 26.11 (3C), 26.09 (3C), 23.6, 22.5, 20.1, 18.40, 18.37, 13.0, 12.7, −4.4, −4.5, −4.6, −4.7; IR (film) ν 3248 (br), 2952, 2856, 1613, 1530, 1456, 1253, 1086, 836, 775 cm^{-1}. HRMS (ESI) m/z calcd for [(M + H)$^+$], 733.5160; found, 733.5152.

(*R*,2*E*,4*E*)-*N*-(2-Aminophenyl)-6-((1*R*,3a*S*,7a*R*,*E*)-4-(2-((3*R*,5*R*)-3,5-dihydroxycyclohexylidene)ethylidene)-7a-methyloctahydro-1*H*-inden-1-yl)-4-methylhepta-2,4-dienamide (5). TBAF (256 μL of a 1 M solution in THF, 0.064 mmol, 4 equiv) and Et_3N (7 μL, 0.048 mmol, 3 equiv) were added to a stirred solution of **8** (12 mg, 0.016 mmol, 1 equiv) in THF (1 mL) under argon, and the mixture was stirred for 48 h. The solution was concentrated in vacuo and loaded directly on to silica gel. Purification by silica gel chromatography (20−60% acetone in hexanes) provided **5** as a clear oil in 62% yield (5 mg, 0.010 mmol). Further purification by reverse phase HPLC (C18, 70/30 MeCN/H_2O) yielded an analytically pure (>97%) sample which was used for biological assays. R_f = 0.5 (60% acetone in hexanes); ^{1}H NMR (400 MHz, $CDCl_3$) δ 7.35 (1H, d, J = 15.2 Hz), 7.27−7.17 (1H, m), 7.15−6.97 (2H, m), 6.80 (1H, d, J = 8.0 Hz), 6.77 (1H, brs), 6.31 (1H, d, J = 11.2 Hz), 5.94 (1H, d, J = 14.8 Hz), 5.84 (1H, d, J = 11.2 Hz), 5.73 (1H, d, J = 10.6 Hz), 4.17−4.08 (1H, m), 4.08−3.99 (1H, m), 3.90 (2H, brs), 2.82 (1H, d, J = 16.0 Hz), 2.72 (1H, dd, J = 12.8, 3.6 Hz), 2.62−2.51 (2H, m), 2.48 (1H, d, J = 13.6 Hz), 2.27−2.14 (4H, m), 1.82 (3H, s), 1.92−1.31 (10H, m), 1.06 (3H, d, J = 6.4 Hz), 0.59 (3H, s); ^{13}C NMR (75 MHz, $CDCl_3$) δ 165.2, 148.3, 142.9, 141.0, 131.6, 129.7, 127.3, 125.3, 124.0, 119.8, 118.5, 117.7, 115.7, 67.6, 67.4, 56.6, 56.3, 46.1, 44.9, 42.4, 40.6, 37.4, 36.2, 29.1, 27.3, 23.7, 22.5, 20.1, 13.0, 12.7; IR (film) ν 3351 (br), 2936, 2871, 1654, 1612, 1528, 1454, 1045, 908, 732 cm^{-1}. HRMS (ESI) m/z calcd for [(M + H)$^+$], 505.3430; found, 505.3424.

VDR Binding and Agonism Assays. VDR binding using a flourescence polarization assay and VDR agonism/antagonism assessed by PCR on CYP24 followed our published procedures.[7] For TSLP, the following primers were used: 5′, -caacttgtagggct; 3′, -gtcgattgaagcga..

HDAC Inhibition. HDAC inibition was measured using a standard fluorometric assay.[8,11]

Chromatin Immunoprecipitation Assay. ChIP assays assessing association of VDR coactivator AIB1 and corepressor NCoR with the promoter of the CYP24 gene were performed eesentially as described.[19] AIB1 and NCoR were immunoprecipitated with ChIP grade antibodies ab2831 and ab24552, respectively, from Abcam (Cambridge, MA).

Molecular Modeling and Dynamics. Initial coordinates of VDR ligand binding domain (LBD) were obtained from the X-ray crystal structure of the VDR-LBD-1α,25(OH)$_2$D$_3$ complex (Protein Data Bank code 1DB1) determined at 1.80 Å resolution.[14] Hydrogen atoms were added, and water molecules were removed. The N(ε)-H tautomer of H397 was selected in accordance with surrounding hydrogen bond network.[14] Next, hydrogen positions were optimized through energy minimization of the VDR-LBD using OPLS_2005 in MacroModel (Maestro 9.0, Schrödinger, Inc.). Ligands **4** and **5** were prepared in Maestro 9.0 (Schrödinger, Inc.) and docked to the full-length and H12-truncated (residues 417−423) VDR-LBD protein. Ten docking runs were performed on the two ligands using the FITTED docking program in the rigid protein mode and SAR option.[13] The structure of **1** cocrystallized with VDR-LBD, and the top-ranking docked poses of **4** and **5** were selected for MD

simulations. These simulations were carried out using the Amber 10 molecular dynamics package following a modified version of the protocol described by Kieltyka et al.[20] Briefly, the atomic charges of the ligands were calculated within the SMART module of FITTED and assigned GAFF[21] atom types. Protein atoms were assigned AMBER atom types and used with the parm99 force field, while ligands were described with GAFF in combination with ad hoc parameters generated for **5** with parmchk. LEaP (Amber 10) was used to combine the initial structure of the VDR-LBD with **1**, **4**, and **5**; to neutralize the system with the addition of sodium cations; and to solvate the whole in a truncated octahedron of TIP3P water molecules with a 10 Å cutoff. The system was energy minimized stepwise, first relaxing the water molecules and ions while keeping all other atoms fixed and then minimizing all atoms. A periodic boundary, constant volume simulation was run over 20 ps with a 1.6 fs time step, keeping the protein and ligands restrained with a 10 kcal·mol^{-1} Å^{-1} harmonic constant, using SHAKE to omit bond stretching involving H atoms and allowing the system to heat up from 0 to 300 K using Langevin dynamics with a collision frequency of 1.0 ps^{-1}. Further 100 ps of simulation at 300K but at constant pressure (1 bar) was performed to relax the system. From then on, 40 ns of unconstrained simulation at otherwise identical conditions as the relaxation was performed, with snapshots saved every 10 ps.

Acknowledgment. This work was supported by Proof of Principle and operating grants to J.H.W. and J.L.G. from the Canadian Institutes of Health Research. J.H.W. is a Chercheur-Boursier National of the Fonds de Recherché en Santé du Québec. M.C.B. thanks the Natural Science and Engineering Research Council of Canada for a predoctoral fellowship.

Supporting Information Available: Scheme for the synthesis of **5**, energies for docked ligands, and additional molecular dynamics structures. This material is available free of charge via the Internet at http://pubs.acs.org.

References

(1) Lin, R.; White, J. H. The pleiotropic actions of vitamin D. *BioEssays* **2004**, *26*, 21–28.
(2) White, J. H. Vitamin D signaling, infectious diseases and regulation of innate immunity. *Infect. Immun.* **2008**, *76*, 3837–3843.
(3) Eeln, G.; Gysemans, C.; Verlinden, L.; Vanoibeek, E.; De Clercq, P.; Van Haver, D.; Mathieu, C.; Bouillon, R.; Verstuyf, A. Mechanisms and potential of the growth inhibitory actions of vitamin D and analogs. *Curr. Med. Chem.* **2007**, *14*, 1893–1910.
(4) Selected examples: (a) Miura, D.; Manabe, K.; Ozono, K.; Saito, M.; Gao, Q.; Norman, A. W.; Ishizuka, S. Antagonistic action of novel 1α,25-dihydroxyvitamin D_3-26,23-lactone analogs on differentiation of human leukemia cells (HL-60) induced by 1α,25-dihydroxyvitamin D_3. *J. Biol. Chem.* **1999**, *274*, 16392–16399. (b) Herdick, M.; Steinmeyer, A.; Carlberg, C. Antagonistic action of a 25-carboxylic ester analogue of 1α,25-dihydroxyvitamin D_3 is mediated by a lack of ligand-induced vitamin D receptor interaction with coactivators. *J. Biol. Chem.* **2000**, *275*, 16506–16512. (c) Herdick, M.; Steinmeyer, A.; Carlberg, C. Carboxylic ester antagonists of 1α,25-dihydroxyvitamin D_3 show cell-specific actions. *Chem. Biol.* **2000**, *7*, 885–894. (d) Kato, Y.; Nakano, Y.; Sano, H.; Tanatani, A.; Kobayashi, H.; Shimazawa, R.; Koshino, H.; Hashimoto, Y.; Nagasawa, K. Synthesis of 1α,25-dihydroxyvitamin D_3-26,23-lactams (DLAMs), a novel series of 1α,25-dihydroxyvitamin D_3 antagonist. *Bioorg. Med. Chem. Lett.* **2004**, *14*, 2579–2583. (e) Saito, N.; Kittaka, A. Highly potent vitamin D receptor antagonists: design, synthesis, and biological evaluation. *ChemBioChem* **2006**, *7*, 1478–1490. (f) Cho, K.; Uneuchi, F.; Kato-Nakamura, Y.; Namekawa, J.-I.; Ishizuka, S.; Takenouchi, K.; Nagasawa, K. Structure−activity relationship studies on vitamin D lactam derivatives as vitamin D receptor antagonist. *Biorg. Med. Chem. Lett.* **2008**, *18*, 4287–4290. (g) Nakabayashi, M.; Yamada, S.; Yoshimoto, N.; Tanaka, T.; Igarashi, M.; Ikura, T.; Ito, N.; Makishima, M.; Tokiwa, H.; Deluca, H. F.; Shimizu, M. Crystal structures of rat vitamin D receptor bound to adamantyl vitamin D analogs: structural basis for vitamin D receptor antagonism and partial agonism. *J. Med. Chem.* **2008**, *51*, 5320–5329. (h) Inaba, Y.; Yoshimoto, N.; Sakamaki, Y.; Nakabayshi, M.; Ikura, T.; Tamamura, H.; Ito, N.; Shimuzu, M.; Yamamoto, K. A new class of vitamin D analogues that induce structural rearrangement of the ligand-binding pocket of the receptor. *J. Med. Chem.* **2009**, *52*, 1438–1449.
(5) Mora, J. R.; Iwata, M.; von Andrian, U. H. Vitamin effects on the immune system: vitamins A and D take centre stage. *Nat. Rev. Immunol.* **2008**, *8*, 685–698.
(6) Iannuzzi, M. C.; Rybicki, B. B.; Tierstein, A. S. Sarcoidosis. *N. Engl. J. Med.* **2007**, *357*, 2153–2165.
(7) Tavera-Mendoza, L. E.; Quach, T.; Dabbas, B.; Hudon, J.; Liao, X.; Palijan, A.; Gleason, J. L.; White, J. H. Incorporation of histone deacetylase inhibition into the structure of a nuclear receptor agonist. *Proc. Nat. Acad. Sci. U.S.A.* **2008**, *105*, 8250–8255.
(8) Lamblin, M.; Dabbas, B.; Spingarn, R.; Mendoza-Sanchez, R.; Wang, T.-T.; An, B.-S.; Huang, D. C.; Kremer, K.; White, J. H.; Gleason, J. L. Vitamin D receptor agonist/histone deacetylase inhibitor molecular hybrids. *Bioorg. Med. Chem.* **2010**, *18*, 4119–4137.
(9) Perlman, K. L.; Sicinski, R. R.; Schnoes, H. K.; DeLuca, H. F. 1α,25-Dihydroxy-19-norvitamin D3, a novel vitamin D-related compound with potential therapeutic activity. *Tetrahedron Lett.* **1990**, *31*, 1823–1824.
(10) Lin, R.; Nagai, Y.; Sladek, R.; Bastien, Y.; Ho, J.; Petrecca, K.; Sotiropoulou, G.; Diamandis, E. P.; Hudson, T.; White, J. H. Expression profiling in squamous carcinoma cells reveals pleiotropic effects of vitamin D3 signaling on cell proliferation, differentiation and immune system regulation. *Mol. Endocrinol.* **2002**, *16*, 1243–1256.
(11) (a) Wegener, D.; Wirsching, F.; Riester, D.; Schwienhorst, A. A fluorogenic histone deacetylase assay well suited for high-throughput activity screening. *Chem. Biol.* **2003**, *10*, 61–68. (b) Wegener, D.; Hildmann, C.; Riester, D.; Schwienhorst, A. Improved fluorogenic histone deacetylase assay for high-throughput-screening applications. *Anal. Biochem.* **2003**, *321*, 202–208.
(12) (a) Peräkylä, M.; Molnár, F.; Carlberg, C. A structural basis for the species-specific antagonism of 26,23-lactones on vitamin D signaling. *Chem. Biol.* **2004**, *11*, 1147–1156. (b) Hashimoto, Y.; Miyachi, H. Nuclear receptor antagonists designed based on the helix-folding inhibition hypothesis. *Bioorg. Med. Chem.* **2005**, *13*, 5080–5093. (c) Yoshimoto, N.; Inaba, Y.; Yamada, S.; Makishima, M.; Shimizu, M.; Yamamoto, K. 2-Methylene 19-nor-25-dehydro-1α-hydroxyvitamin D_3 26,23-lactones: synthesis, biological activities and molecular basis of passive antagonism. *Bioorg. Med. Chem.* **2008**, *16*, 457–473.
(13) (a) Corbeil, C. R.; Englebienne, P.; Moitessier, N. Docking ligands into flexible and solvated macromolecules. 1. Development and validation of FITTED 1.0. *J. Chem. Inf. Model.* **2007**, *47*, 435–449. (b) Corbeil, C. R.; Englebienne, P.; Moitessier, N. Docking ligands into flexible and solvated macromolecules. 2. Development and application of FITTED 1.5 to the virtual screening of potential HCV polymerase inhibitors. *J. Chem. Inf. Model.* **2008**, *48*, 902–909. (c) Corbeil, C. R.; Moitessier, N. Docking ligands into flexible and solvated macromolecules. 3. Impact of input ligand conformation, protein flexibility, and water molecules on the accuracy of docking programs. *J. Chem. Inf. Model.* **2009**, *49*, 997–1009.
(14) Rochel, N.; Wurtz, J. M.; Mitschler, A.; Klaholz, B.; Moras, D. The crystal structure of the nuclear receptor for vitamin D bound to its natural ligand. *Mol. Cell* **2000**, *5*, 173–179.
(15) Bourguet, W.; Germain, P.; Gronemeyer, H. Nuclear receptor ligand-binding domains: three-dimensional structures, molecular interactions and pharmacological implications. *Trends Pharmacol. Sci.* **2000**, *21*, 381–388.
(16) Graphics prepared in the PyMOL Molecular Graphics System, version 1.2r2pre, from Schrödinger, LLC.
(17) Feng, W.; Ribeiro, R. C. J.; Wagner, R. L.; Nguyen, H.; Apriletti, J. W.; Fletterick, R. J.; Baxter, J. D.; Kushner, P. J.; West, B. L. Hormone-dependent coactivator binding to a hydrophobic cleft on nuclear receptors. *Science* **1998**, *280*, 1747–1749.
(18) Peräkylä, M. *Lect. Notes Comput. Sci.* (including subseries Lect. Notes Artif. Intell. and Lect. Notes Bioinf.) **2007**, *4699*, 82−89.
(19) Wang, T.-T.; Nestel, F. P.; Bourdeau, V.; Nagai, Y.; Wang, Q.; Liao, J.; Tavera-Mendoza, L.; Lin, R.; Hanrahan, J. H.; Mader, S.; White, J. H. 1,25-Dihydroxyvitamin D3 directly stimulates antimicrobial peptide gene transcription. *J. Immunol.* **2004**, *173*, 2909–2912.
(20) Kieltyka, R.; Englebienne, P.; Moitessier, N.; Sleiman, H. Quantifying interactions between G-quadruplex DNA and transition metal complexes. *Methods Mol. Biol.* **2010**, *608*, 223–255.
(21) Wang, J.; Wolf, R. M.; Caldwell, J. W.; Kollman, P. A.; Case, D. A. Development and testing of a general amber force field. *J. Comput. Chem.* **2004**, *25*, 1157–1174.